

Surface critical behavior of driven diffusive systems with open boundaries

K. Oerding and H. K. Janssen
Institut für Theoretische Physik III
Heinrich-Heine-Universität
D-40225 Düsseldorf, Germany
(July 9, 2017)

Using field theoretic renormalization group methods we study the critical behavior of a driven diffusive system near a boundary perpendicular to the driving force. The boundary acts as a particle reservoir which is necessary to maintain the critical particle density in the bulk. The scaling behavior of correlation and response functions is governed by a new exponent η_1 which is related to the anomalous scaling dimension of the chemical potential of the boundary. The new exponent and a universal amplitude ratio for the density profile are calculated at first order in $\epsilon = 5 - d$. Some of our results are checked by computer simulations.

PACS: 05.40.+j, 05.70.Fh, 64.60.Ak, 66.30.Dn, 72.70.+m

I. INTRODUCTION

In order to study the properties of thermodynamic systems far from equilibrium physicists have been looking for simple models which capture the main features of non-equilibrium phenomena. Driven diffusive systems (DDS) introduced by Katz et. al. [1] to model fast ionic conductors are characterized by a particles conserving dynamics and a stationary state which does not satisfy detailed balance. Their study has led to the discovery of the connection between the validity of a conservation law and the existence of long-range spatial correlations in non-equilibrium steady states.

A simple microscopic realization of DDS is an Ising lattice gas with attractive nearest neighbor interaction and an external driving force E which prefers particle jumps in the direction parallel to E [1,2]. The strength of the particle attraction can be varied by a temperature-like parameter T . Below a critical value $T_c(E)$ particles are separated in the stationary state into regions of high and low densities, where the interfaces are oriented parallel to the driving force (for $E \neq 0$). The phase transition at $T_c(E)$ is second order. For an infinite driving force particle jumps in the direction antiparallel to E are suppressed. In this case the phase transition occurs at $T_c(\infty) \approx 1.41 T_c(0)$, where $T_c(0)$ is the critical temperature of the two dimensional Ising model [2]. The critical behavior of this system has been extensively studied by Monte Carlo simulations and renormalization group methods [3]. (For a recent review see [4].)

In most studies of DDS periodic boundary conditions in all directions are imposed to avoid surface effects. In this case the particles are driven along a ring or torus. In more realistic models particles are fed into the system at one side and extracted at the other. The asymmetric exclusion model [5] is a DDS with hard core repulsion (but without nearest neighbor interaction, i.e. $T = \infty$). The density profile in a one-dimensional exclusion model with a particle source and a sink was investigated numerically by Krug [6]. His results were later confirmed and generalized by exact calculations [7–9]. An impor-

tant result of these works is the ‘maximum current principle’ which states the following: If the system is placed between two particle reservoirs A and B (with the respective densities c_A and c_B with $c_A \geq c_B$) and the driving force points from A to B, then the bulk density takes the value c_{\max} which maximizes the current j under the constraint $c_A \geq c \geq c_B$, i.e.

$$j(c_{\max}) = \max\{j(c) \mid c_A \geq c \geq c_B\}. \quad (1)$$

The maximum current density of an Ising lattice gas with attractive particle-particle interaction equals its critical density $1/2$. The low temperature phase of this system with open boundaries in two dimensions has been studied by Boal et. al. [10].

In the present paper field theoretic renormalization group methods are employed to investigate the effects of open boundaries on DDS at the critical point $T_c(E)$. We assume that a plane particle source A perpendicular to the driving force is located at the left boundary of the system (coordinate $z = 0$) and impose periodic boundary conditions in the transverse directions. The effect of the particle source is to suppress density fluctuations and to maintain a constant density c_A at $z = 0$. The particles are extracted from the system when they reach a sink B located at $z = L$ ($L \rightarrow \infty$).

It is well known that in physical systems with long ranged correlations the influence of a surface extends far into the bulk. The critical behavior near a boundary is governed by universal scaling laws with critical exponents that (in general) cannot be expressed in terms of bulk exponents (a review is given in Ref. [11]). The applicability of renormalization group methods to investigate both static [11–15] and dynamic [16–18] surface universality classes is well established. Especially encouraging are the results of Ref. [19] where this technique has been used to obtain an approximate profile for one-dimensional DDS with open boundaries. It turned out that the profile calculated by renormalization group improved perturbation theory (at one-loop order) was in good agreement with the exact result of Ref. [7].

In the next section the semi-infinite extension of the field theoretic model for DDS at the critical point (introduced in [3]) is presented. Above the upper critical dimension $d_c = 5$ of this model fluctuations around the mean field profile can be treated by naïve perturbation theory. The mean field profile and Gaussian fluctuations for $d > 5$ are considered in some detail in Secs. III and IV since the results of this analysis remain qualitatively valid for $d < 5$. In Sec. V the renormalization group is used to obtain the scaling behavior of Green functions and the density profile below five dimensions. Sec. VII contains a discussion.

II. THE MODEL

The analysis in the present paper is based on the field theoretic model introduced by Janssen and Schmittmann [3] to study the critical behavior of a diffusive system with a single conserved density subjected to an external driving force. The model can be written in the form of the continuity equation

$$\partial_t s + \nabla_{\perp} \mathbf{j}_{\perp} + \partial_{\parallel} j_{\parallel} = 0, \quad (2)$$

where $s(\mathbf{r}, t) = c(\mathbf{r}, t) - \bar{c}$ denotes the deviation of the concentration from its average (bulk) value \bar{c} , and \mathbf{j}_{\perp} and j_{\parallel} are the respective components of the current perpendicular and parallel to the driving force. The explicit expression for the current can be motivated by the following symmetry requirements [4]:

- (i) Isotropy with respect to the $(d - 1)$ -dimensional transverse subspace,
- (ii) invariance of the equation of motion under reversal of the driving force ($E \leftrightarrow -E$) and particle-hole exchange ('charge conjugation', $s \leftrightarrow -s$),
- (iii) invariance under force reversal and reflection in r_{\parallel} (the coordinate parallel to the force).

A continuum model satisfying (i)–(iii) describes, for instance, the long time and large distance behavior of a driven Ising lattice gas at its critical density $1/2$. Since the current in this system is at its maximum value for half filling one may use the maximum current principle (in a system with open boundaries) to adjust the bulk density to the critical value.

Keeping only terms which are consistent with the above conditions (i)–(iii) and relevant or marginal in the renormalization group sense the current may be written (upon rescaling of s) in the form

$$j_{\perp} = \nabla_{\perp} [-\lambda(\tau s - \Delta_{\perp} s) + \zeta], \quad (3a)$$

$$j_{\parallel} = E(\sigma_0 + \sigma_2 s^2) - \lambda \rho \partial_{\parallel} s, \quad (3b)$$

where ζ is a Gaussian random force with the correlation

$$\langle \zeta(\mathbf{r}, t) \zeta(\mathbf{r}', t') \rangle = 2\lambda \delta(\mathbf{r} - \mathbf{r}') \delta(t - t'). \quad (3c)$$

The third order derivative in Eq. (3a) has to be kept because the coefficient τ of the first order derivative vanishes at the critical point (transverse phase transition [3]). The coefficient σ_0 may be interpreted as the conductivity of the system at the maximum current density \bar{c} . Deviations from \bar{c} due to fluctuations or a non-constant density profile decrease the current. This effect is modeled by the term $E\sigma_2 s^2$ in Eq. (3b). The coefficient τ measures the deviation of the temperature parameter from its critical value and ρ takes into account the anisotropy of the diffusion constant. Even if the diffusion constant is isotropic ($\rho = 1$) in the original Langevin equation it becomes anisotropic under coarse graining.

For the subsequent field theoretic analysis it is convenient to recast the model in the form of the dynamic functional [20–24,3]

$$\begin{aligned} \mathcal{J}_b[\tilde{s}, s] = \int dt \int_V d^d r \left\{ \tilde{s} \partial_t s + \lambda [(\Delta_{\perp} \tilde{s})(\Delta_{\perp} s) \right. \\ \left. + \tau (\nabla_{\perp} \tilde{s})(\nabla_{\perp} s) + \rho (\partial_{\parallel} \tilde{s})(\partial_{\parallel} s) \right. \\ \left. + \frac{1}{2} g (\partial_{\parallel} \tilde{s}) s^2 - h \partial_{\parallel} \tilde{s} - (\nabla_{\perp} \tilde{s})^2 \right\}, \end{aligned} \quad (4)$$

where $\lambda g \sim -E\sigma_2$, and \tilde{s} is a Martin–Siggia–Rose response field [25]. While the functional (4) allows us to calculate response and correlation functions for an infinite bulk system the influence of the boundaries has to be modeled by additional surface contributions. If the boundary is perpendicular to the driving force the region of integration in Eq. (4) is the half space $V = \{(\mathbf{r}_{\perp}, z) \mid \mathbf{r}_{\perp} \in \mathbf{R}^{d-1}, z \geq 0\}$, and the surface is defined by $z = 0$. Omitting irrelevant and redundant terms [19] the surface functional reads

$$\begin{aligned} \mathcal{J}_s[\tilde{s}, s] = \int dt \int_{\partial V} d^{d-1} r_{\perp} \lambda \left(c \tilde{s} s - \tilde{c} \tilde{s}^2 - c_2 \tilde{s} \Delta_{\perp} s \right. \\ \left. + \frac{1}{2} g_s \tilde{s} s^2 - h_s \tilde{s} \right) \end{aligned} \quad (5)$$

Response and correlation functions can now be calculated by functional integration with the weight $\exp(-\mathcal{J})$, where $\mathcal{J} = \mathcal{J}_b + \mathcal{J}_s$.

III. EQUATION OF MOTION AND MEAN FIELD APPROXIMATION

An exact equation for the stationary profile $\Phi(z) = \langle s(\mathbf{r}, t) \rangle$ follows from the invariance of the generating functional

$$\begin{aligned} Z[\tilde{J}, J; \tilde{J}_1, J_1] = \int \mathcal{D}[\tilde{s}, s] \exp \left(-\mathcal{J}_b[\tilde{s}, s] - \mathcal{J}_1[\tilde{s}_s, s_s] \right. \\ \left. + (\tilde{J}, \tilde{s}) + (J, s) + (\tilde{J}_1, \tilde{s}_s) + (J_1, s_s) \right) \end{aligned} \quad (6)$$

under an infinitesimal shift of the field \tilde{s} . In Eq. (6) $s_s(\mathbf{r}_{\perp}) = s(\mathbf{r}_{\perp}, 0)$ denotes the field at the surface and the abbreviations

$$(\tilde{J}, \tilde{s}) = \int dt \int_V d^d r \tilde{J} \tilde{s} \quad (7)$$

and

$$(J_1, s_s) = \int dt \int_{\partial V} d^{d-1} r_{\perp} J_1 s_s \quad (8)$$

have been used. The invariance of $Z[\tilde{J}, J; \tilde{J}_1, J_1]$ implies the equation of motion

$$\partial_t s + \lambda [(\Delta_{\perp} - \tau) \Delta_{\perp} s - \partial_{\parallel} (\rho \partial_{\parallel} s + \frac{1}{2} g s^2) + 2 \Delta_{\perp} \tilde{s}] = \tilde{J} \quad (9)$$

which holds after insertion into averages. The invariance of $Z[\tilde{J}, J; \tilde{J}_1, J_1]$ under a shift of the surface field \tilde{s}_s leads to the equation of motion

$$\begin{aligned} -\rho \partial_n s - \frac{g - g_s}{2} s_s^2 + c s_s - 2 \tilde{c} \tilde{s}_s \\ - c_2 \Delta_{\perp} s_s - h_s + h = \frac{1}{\lambda} \tilde{J}_1 \end{aligned} \quad (10)$$

which fixes the boundary condition. Taking the average on both sides of (9) for vanishing sources $\tilde{J} = J = \tilde{J}_1 = J_1 = 0$ one obtains

$$\partial_z [\rho \partial_z \Phi(z) + \frac{1}{2} g (\Phi(z)^2 + C(z))] = 0 \quad (11)$$

or, since $\Phi_{\text{bulk}} = 0$ due to the definition of s ,

$$\Phi'(z) + \frac{g}{2\rho} (\Phi(z)^2 + C(z) - C_{\text{bulk}}) = 0. \quad (12)$$

The function $C(z) = \langle [s(\mathbf{r}_{\perp}, z; t) - \Phi(z)]^2 \rangle$ describes density fluctuations at the distance z from the surface and C_{bulk} denotes its value for $z \rightarrow \infty$.

In the mean field approximation one neglects the correlation function $C(z)$ and obtains for the profile

$$\Phi_{\text{mf}}(z) = \Phi_0 \left(1 + \frac{g}{2\rho} \Phi_0 z \right)^{-1}. \quad (13)$$

Dimensional analysis shows that the momentum dimension of the coupling coefficient g is given by $[g] = (5 - d)/2$, and the mean field approximation breaks down below the upper critical dimension $d_c = 5$. For $d > 5$ corrections to the mean field profile can be obtained by naïve perturbation theory. At lowest order it is sufficient to calculate the perturbation $C(z) - C_{\text{bulk}}$ in Eq. (12) by a Gaussian approximation.

IV. CORRECTIONS TO THE MEAN FIELD PROFILE FOR $D > 5$

In the simplest case, $\Phi_{\text{mf}}(z) = \Phi_0 = h_s = 0$, the Fourier transform (with respect to \mathbf{r}_{\perp} and t) of the Gaussian propagator

$$G(\mathbf{r}_{\perp}, z, z'; t) = \langle s(\mathbf{r}_{\perp}, z; t) \tilde{s}(\mathbf{0}, z'; 0) \rangle_0 \quad (14)$$

is given by [19]

$$\begin{aligned} \hat{G}_{\mathbf{q}_{\perp}, \omega}(z, z') = \frac{1}{2\lambda\sqrt{\rho}\kappa} \left[e^{-\kappa|z-z'|/\sqrt{\rho}} \right. \\ \left. + \frac{\kappa - c/\sqrt{\rho}}{\kappa + c/\sqrt{\rho}} e^{-\kappa(z+z')/\sqrt{\rho}} \right] \end{aligned} \quad (15)$$

with

$$\kappa = \left(\frac{i\omega}{\lambda} + q_{\perp}^2 (\tau + q_{\perp}^2) \right)^{1/2}. \quad (16)$$

The parameter c occurring in the surface functional \mathcal{J}_1 and in the propagator describes (for $c > 0$) the suppression of density fluctuations by the particle reservoir at the boundary. Since the momentum dimension of c is one the asymptotic scaling behavior is governed by the fixed point $c_{\star} = \infty$. At this fixed point the fields \tilde{s} and s satisfy the Dirichlet boundary conditions $\tilde{s}_s = s_s = 0$.

The Fourier transform of the Gaussian correlation function

$$C(\mathbf{r}_{\perp}, z, z'; t) = \langle s(\mathbf{r}_{\perp}, z; t) s(\mathbf{0}, z'; 0) \rangle_0 \quad (17)$$

at the Dirichlet fixed point $c_{\star} = \infty$ can be derived from the Gaussian part of the dynamic functional. This calculation yields

$$\begin{aligned} \hat{C}_{\mathbf{q}_{\perp}, \omega}(z, z') = 2\lambda q_{\perp}^2 \int_0^{\infty} dz'' \hat{G}_{\mathbf{q}_{\perp}, \omega}(z, z'') \hat{G}_{\mathbf{q}_{\perp}, -\omega}(z'', z') \\ = -\frac{2\lambda q_{\perp}^2}{\omega} \Im[\hat{G}_{\mathbf{q}_{\perp}, \omega}(z, z')], \end{aligned} \quad (18)$$

where $\Im[\dots]$ denotes the imaginary part. The equal-time correlation function at the point (\mathbf{r}_{\perp}, z) is given by

$$\begin{aligned} C(z) = \int_{\mathbf{q}_{\perp}, \omega} \hat{C}_{\mathbf{q}_{\perp}, \omega}(z, z) \\ = C_{\text{bulk}} - \frac{1}{2\sqrt{\rho}} (8\pi z / \sqrt{\rho})^{-(d-1)/2} \end{aligned} \quad (19)$$

with $C_{\text{bulk}} \sim \Lambda^{d-1}/\sqrt{\rho}$ (where Λ is a cut-off wave number).

We can now use Eqs. (12) and (19) to compute the fluctuation correction to the constant mean field profile $\Phi_{\text{mf}}(z) = 0$. At first order in g we get

$$\Phi^{[1]}(z) = -\frac{g(8\pi)^{-(d-1)/2}}{2(d-3)\rho} \left(\frac{z}{\sqrt{\rho}} \right)^{-(d-3)/2}. \quad (20)$$

One can easily check by dimensional analysis that higher order corrections to the profile decay as $\Phi^{[2n+1]}(z)/\Phi^{[1]}(z) \sim z^{-n(d-5)/2}$ (up to cut-off dependent terms which may change the amplitude of the leading term proportional to $z^{-(d-3)/2}$).

In the limit $c, h_s \rightarrow \infty$ (with $h_s/c =: h_1$ fixed) the boundary value of the mean field profile is given by $\Phi_0 =$

h_1 . This follows from Eqs. (10) and (13). For $\Phi_0 > 0$ the mean field profile decays asymptotically as $\Phi_{\text{mf}}(z) \simeq 2\rho/(gz)$, and the fluctuation correction $\sim z^{-(d-3)/2}$ can be neglected for $z \rightarrow \infty$ ($d > 5$). However, if h_1 is positive but small the profile $\Phi(z)$ is negative for $z < \zeta$, where $\zeta = \zeta(h_1)$ is a crossover length. The dependence of the profile on the boundary chemical potential h_1 is depicted qualitatively in Fig. 1. The crossover length ζ tends to infinity for $h_1 \rightarrow 0^+$. To estimate ζ for small h_1 we equate the mean field profile $\Phi_{\text{mf}}(\zeta)$ with the fluctuation term $\zeta^{-(d-3)/2}$ and obtain

$$\zeta \sim h_1^{-2/(d-3)} \quad (21)$$

for $h_1 \rightarrow 0^+$, $d > 5$.

In the language of semi-infinite magnetic systems the case $h_1 = \infty$ corresponds to the normal transition and $h_1 = 0$ is the ordinary point. A length scale similar to ζ has already been found in magnetic systems near the ordinary transition [26,27]. There the length scale ζ characterizes the magnetization profile induced by a small magnetic surface field.

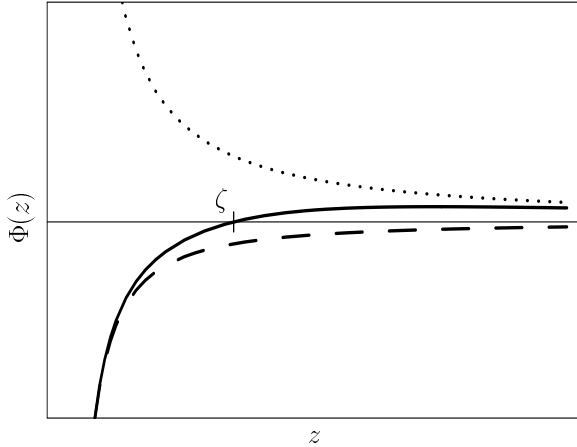


FIG. 1. Sketch of the profile $\Phi(z)$ for $h_1 = \infty$ (dotted), $h_1 > 0$ finite (solid curve), and $h_1 = 0$ (dashed). For $h_1 < 0$ the density in the bulk stays below its critical value indicated by the horizontal line.

V. RENORMALIZATION GROUP ANALYSIS

A. Renormalization

The naïve perturbation theory described in the previous section breaks down below the upper critical dimension $d_c = 5$. The renormalization group allows us to improve the perturbation expansion by a partial resummation.

Since the individual terms of the perturbation series contain for $d = d_c$ ultraviolet divergent integrals a regularization prescription is required to obtain well-defined expressions for the otherwise infinite integrals. Here we

use the dimensional regularization method (analytic continuation of the integrals as functions of d). The remaining poles in $\epsilon = d_c - d$ are then absorbed into reparametrizations of the coupling coefficients and the fields. In the field theory for the bulk model (without a surface) a renormalization of the parameter $\rho = Z\rho_R$ is sufficient to cancel the ultraviolet divergences at every order of the perturbation theory [3]. At one-loop order the renormalization factor is given by

$$Z = 1 - \frac{u}{\epsilon} + O(u^2), \quad u = A_\epsilon g^2 \rho_R^{-3/2} \mu^{-\epsilon}, \quad (22)$$

where μ is an external momentum scale and the geometrical factor $A_\epsilon = (3/4)(4\pi)^{-d/2}\Gamma((3-\epsilon)/2)\Gamma(1+\epsilon/2)/\Gamma(2-\epsilon/2)$ has been introduced for convenience. (The index ‘ R ’ indicates renormalized quantities.)

In order to investigate the scaling behavior of response functions near the boundary one has to calculate Green functions with insertions of the surface response field \tilde{s}_s . Since the Gaussian propagator (15) vanishes at the Dirichlet fixed point $c_* = \infty$ it is necessary to go to higher orders in c^{-1} to obtain non-trivial results [11,12,28]. At first order in c^{-1} the propagator becomes (for $z' = 0$)

$$\hat{G}_{\mathbf{q}_\perp, \omega}(z, 0) = \frac{1}{c} \rho \partial_{z'} \hat{G}_{\mathbf{q}_\perp, \omega}^{(D)}(z, z') \Big|_{z'=0} + \dots, \quad (23)$$

where $\hat{G}_{\mathbf{q}_\perp, \omega}^{(D)}(z, z')$ denotes the propagator (15) for $c = \infty$. This shows that the leading order terms in an expansion in powers of c^{-1} can be studied in the framework of a field theory with Dirichlet boundary conditions after replacing in expectation values

$$\tilde{s}_s \rightarrow c^{-1} \rho \partial_n \tilde{s}. \quad (24)$$

Analogously insertions of the surface field s_s have to be replaced (at leading order) by the the normal derivative $c^{-1} \rho \partial_n s$.

Since a boundary breaks the translational invariance of the system it gives rise to new divergences in the perturbation series which are located at the surface [i.e., proportional to $\delta(z)$]. These surface divergences have to be subtracted by appropriate counter terms added to the dynamic functional \mathcal{J} . In the appendix it is shown that the required counter terms have the form

$$\mathcal{J}_{\text{bct}}[\tilde{s}, s] = \int dt \int_V d^d r \lambda [\rho_R (Z - 1) (\partial_\parallel \tilde{s}) (\partial_\parallel s) + \rho_R^{-1/2} A_\epsilon g \mu^{-\epsilon} A \tau^2 \partial_\parallel \tilde{s}] \quad (25)$$

to remove bulk divergences and

$$\mathcal{J}_{\text{sct}}[\tilde{s}, s] = \int dt \int_{\partial V} d^{d-1} r_\perp \lambda [\rho_R^{-1/2} A_\epsilon g \mu^{-\epsilon} K (\rho \partial_n^2 \tilde{s}) + B (\rho \partial_n \tilde{s}) s_s + \rho_R^{-1} A_\epsilon g \mu^{-\epsilon} F \tau (\rho \partial_n \tilde{s})] \quad (26)$$

to cancel ϵ -poles located at the surface. The renormalization parameters A, B, F, K are calculated at one-loop order with the result

$$A = -\frac{1}{\epsilon} \quad B = -\frac{u}{3\epsilon} \quad F = -\frac{4}{3\epsilon} \quad K = \frac{2}{3\epsilon}. \quad (27)$$

The first term in \mathcal{J}_{bct} renormalizes the diffusion coefficient ρ . The bulk counter term proportional to $\partial_{\parallel}\tilde{s}$ corresponds to a renormalization of the bulk current [29]

$$h = h_R - \rho_R^{-1/2} A_{\epsilon} g \mu^{-\epsilon} A \tau^2. \quad (28)$$

We now show that the surface counter terms proportional to the operators $(\rho\partial_n\tilde{s})s_s$ and $\rho\partial_n^2\tilde{s}$ can be replaced by a multiplicative renormalization of the surface response field $\rho\partial_n\tilde{s}$. In order to study single insertions of $(\rho\partial_n\tilde{s})s_s$ and $\rho\partial_n^2\tilde{s}$ in Feynman diagrams we first connect them to the Gaussian response function $\hat{G}_{\mathbf{q}_{\perp},\omega}^{(D)}(z, z')$, i.e. we calculate the Gaussian expectation values

$$\left\langle s(z)\tilde{s}(z') \int dt' \int d^{d-1}x' \lambda(\rho\partial_n\tilde{s})s_s \right\rangle_0 = 0, \quad (29)$$

$$\begin{aligned} \left\langle s(z)(\rho\partial_n\tilde{s}) \int dt' \int d^{d-1}x' \lambda(\rho\partial_n\tilde{s})s_s \right\rangle_0 \\ = \frac{1}{\lambda} e^{-\kappa z/\sqrt{\rho}} = \langle s(z)(\rho\partial_n\tilde{s}) \rangle_0 \end{aligned} \quad (30)$$

and

$$\left\langle s(z) \int d^{d-1}x' \lambda \rho \partial_n^2 \tilde{s} \right\rangle_0 = -\delta(z). \quad (31)$$

In Eqs. (30) and (31) the vertices with normal derivatives have to be interpreted as

$$\lambda(\rho\partial_n\tilde{s})s_s = \lim_{z \rightarrow 0} \lambda(\rho\partial_{\parallel}\tilde{s}(z))s_s(z) \quad (32a)$$

and

$$\lambda\rho\partial_n^2\tilde{s} = \lim_{z \rightarrow 0} \lambda\rho\partial_{\parallel}^2\tilde{s}(z), \quad (32b)$$

respectively, where the limit $z \rightarrow \infty$ has to be taken *after* the averages $\langle \dots \rangle_0$ have been performed [11,30].

Equations (29) and (30) show that the counter term $B\lambda(\rho\partial_n\tilde{s})s_s$ has an effect only in diagrams in which it is connected to the surface response field $\rho\partial_n\tilde{s}$. In Green functions with an insertion of $\rho\partial_n\tilde{s}$ it effectively replaces $\rho\partial_n\tilde{s}$ with $(1-B)\rho\partial_n\tilde{s}$.

If the argument of s on the l.h.s. of Eq. (31) is fixed (with $z > 0$) the average in (31) vanishes. However, due to the δ -function one obtains a non-zero result if Eq. (31) is integrated over z . Such an integration occurs in the calculation of the Feynman diagram shown in Fig. 2, where the counter term vertex proportional to $\lambda\rho\partial_n^2\tilde{s}$ is connected to the bulk vertex g . Fig. 2 shows that an insertion of the counter term

$$\lambda\rho_R^{-1/2} A_{\epsilon} g \mu^{-\epsilon} K \rho \partial_n^2 \tilde{s}$$

in a Feynman diagram has the same effect as the vertex $uK\lambda\rho_R(\partial_n\tilde{s})s_s$.

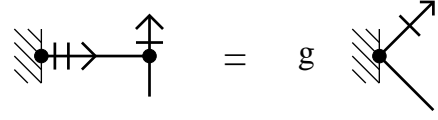


FIG. 2. Effect of the vertex $\lambda\rho\partial_n^2\tilde{s}$ in a Feynman diagram. The hatched area represents the boundary $z = 0$. Each short line perpendicular to a propagator line indicates a derivative with respect to z .

The above analysis shows that the counter terms proportional to $\rho\partial_n^2\tilde{s}$ and $(\rho\partial_n\tilde{s})s_s$ give at one-loop order rise to a renormalization of the surface response field

$$[\rho\partial_n\tilde{s}]_R = Z_1^{-1/2} \rho\partial_n\tilde{s}, \quad (33)$$

where

$$Z_1^{-1/2} = 1 - B - uK + O(u^2) = 1 - \frac{u}{3\epsilon} + O(u^2). \quad (34)$$

The relation between the redundant surface couplings (here B, K) and Z_1 can be extended to higher orders in u in a similar way as in the case of the ϕ^4 -model [30].

The last counter term in \mathcal{J}_{sct} which couples to $\rho\partial_n\tilde{s}$ renormalizes the surface chemical potential

$$h_1 = Z_1^{-1/2} ([h_1]_R - \rho_R^{-1} A_{\epsilon} g \mu^{-\epsilon} F \tau). \quad (35)$$

B. Scaling

With the renormalizations at hand we are in a position to determine the scaling behavior of the Green functions

$$\begin{aligned} G_{\tilde{N},\tilde{N}}^{\tilde{M},M}(\{\mathbf{r}, \mathbf{x}, t\}) = \left\langle \prod_{i=1}^{\tilde{N}} \tilde{s}(\tilde{\mathbf{r}}_i, \tilde{t}_i) \prod_{j=1}^N s(\mathbf{r}_j, t_j) \right. \\ \left. \times \prod_{k=1}^{\tilde{M}} \rho\partial_n\tilde{s}(\tilde{\mathbf{x}}_k, \tilde{t}_{sk}) \prod_{l=1}^M \rho\partial_n s(\mathbf{x}_l, t_{sl}) \right\rangle^{\text{(conn)}}. \end{aligned} \quad (36)$$

with \tilde{M} insertions of the surface response field $\rho\partial_n\tilde{s}$ and M insertions of $\rho\partial_n s$. In this subsection we omit the index ‘ R ’ since only renormalized quantities are used.

At the critical point $\tau = h = 0$ the Green functions satisfy the renormalization group equation

$$\begin{aligned} \left[\mu \frac{\partial}{\partial \mu} + \beta(u) \frac{\partial}{\partial u} + \zeta(u) \rho \frac{\partial}{\partial \rho} + \frac{1}{2} \gamma_1(u) h_1 \frac{\partial}{\partial h_1} \right. \\ \left. + \frac{\tilde{M}}{2} \gamma_1(u) \right] G_{\tilde{N},\tilde{N}}^{\tilde{M},M}(\{\mathbf{r}, \mathbf{x}, t\}; u, \rho, h_1; \lambda, \mu) = 0 \end{aligned} \quad (37)$$

which follows from the independence of the unrenormalized Green functions from the momentum scale μ . The Wilson functions are given by

$$\zeta(u) = \mu \left. \frac{d \ln \rho}{d \mu} \right|_0 = -u + O(u^2), \quad (38a)$$

$$\beta(u) = \mu \left. \frac{d u}{d \mu} \right|_0 = u \left(-\epsilon - \frac{3}{2} \zeta(u) \right), \quad (38b)$$

$$\gamma_1(u) = \mu \left. \frac{d \ln Z_1}{d \mu} \right|_0 = -\frac{2}{3} u + O(u^2), \quad (38c)$$

where the derivatives are calculated at fixed bare parameters.

The renormalization group equation (37) can be solved by the method of characteristics with the result

$$G_{\bar{N}, \bar{N}}^{\bar{M}, \bar{M}}(\{\mathbf{r}, \mathbf{x}, t\}; u, \rho, h_1; \lambda, \mu) = X_1(l)^{\bar{M}/2} \times G_{\bar{N}, \bar{N}}^{\bar{M}, \bar{M}}(\{\mathbf{r}, \mathbf{x}, t\}; \bar{u}(l), X(l)\rho, X_1(l)^{1/2}h_1; \lambda, \mu l). \quad (39)$$

The functions $\bar{u}(l)$, $X(l)$, and $X_1(l)$ are solutions of the set of ordinary differential equations

$$\frac{d\bar{u}(l)}{d \ln l} = \beta(\bar{u}(l)), \quad \bar{u}(1) = u, \quad (40a)$$

$$\frac{d \ln X(l)}{d \ln l} = \zeta(\bar{u}(l)), \quad X(1) = 1, \quad (40b)$$

$$\frac{d \ln X_1(l)}{d \ln l} = \gamma_1(\bar{u}(l)), \quad X_1(1) = 1. \quad (40c)$$

In the limit $l \rightarrow 0$ the scale dependent coupling coefficient $\bar{u}(l)$ tends to the fixed point value $u_* = (2/3)\epsilon + O(\epsilon^2)$ and the Green functions display power law scaling with

$$X(l) \simeq X_* l^{-2\eta}, \quad \eta = -\frac{1}{2} \zeta(u_*) = \frac{5-d}{3}, \quad (41)$$

$$X_1(l) \simeq X_{1,*} l^{\eta_1}, \quad \eta_1 = \gamma_1(u_*) = -\frac{4\epsilon}{9} + O(\epsilon^2). \quad (42)$$

The amplitudes X_* and $X_{1,*}$ are not universal.

Eq. (39) can be further simplified by dimensional analysis. The momentum dimensions of r_\perp , r_\parallel , t , \bar{s} , s , and h_1 follow from the form of the functional \mathcal{J} (which has to be dimensionless) and are given by

$$\begin{aligned} r_\perp &\sim \mu^{-1}, & r_\parallel &\sim \rho^{1/2} \mu^{-2}, & t &\sim \lambda^{-1} \mu^{-4}, \\ \bar{s} &\sim \rho^{-1/4} \mu^{(d+3)/2}, & s &\sim h_1 \sim \rho^{-1/4} \mu^{(d-1)/2}, \end{aligned} \quad (43)$$

respectively. For small l Eq. (39) maps the large length and time scales of the critical region on scales on which Green functions can be calculated perturbatively. Here we are especially interested in the profile $\Phi(z) = G_{0,1}^{0,0}(z)$. Choosing for the flow parameter the value

$$l = \left(\frac{\mu^2 z}{\sqrt{\rho} X_*} \right)^{-1/(2+\eta)} \rightarrow 0 \quad (44)$$

we obtain from Eq. (39) in conjunction with dimensional analysis the scaling form

$$\Phi(z, h_1) = a z^{-\sigma} F(b h_1 z^{1/\nu_1}), \quad (45)$$

with the exponents

$$\sigma = \frac{d-1+\eta}{2(2+\eta)} = \frac{1+d}{11-d} \quad (46)$$

and

$$\frac{1}{\nu_1} = \frac{d-1+\eta-\eta_1}{2(2+\eta)} = 1 - \frac{2\epsilon}{9} + O(\epsilon^2). \quad (47)$$

In (45) a and b are non-universal scale factors while the scaling function F is universal.

C. A universal amplitude ratio

We know from the discussion of the mean field profile and the fluctuation corrections in section IV that $\Phi(z, h_1)$ is finite and non-zero in both cases $h_1 = \infty$ and $h_1 = 0$. It therefore makes sense to define the universal amplitude ratio

$$D = \lim_{z \rightarrow \infty} \frac{\Phi(z, 0)}{\Phi(z, \infty)} = \frac{F(0)}{F(\infty)}. \quad (48)$$

A perturbative calculation based on the results of section IV yields

$$\begin{aligned} \frac{\Phi(z, 0)}{\Phi(z, \infty)} &= -\frac{g^2 (8\pi)^{-(d-1)/2}}{4(d-3)\rho^{3/2}} \left(\frac{z}{\sqrt{\rho}} \right)^{\epsilon/2} + O(g^4) \\ &= -\frac{u}{6} + O(u^2, u\epsilon). \end{aligned} \quad (49)$$

Upon application of the renormalization group transformation with the choice (44) for the flow parameter this becomes

$$D = -\frac{\epsilon}{9} + O(\epsilon^2). \quad (50)$$

In the upper critical dimension $d = 5$ the solution of the flow equation (40a) reads

$$\bar{u}(l) \simeq \frac{2}{3 \ln(1/l)} \quad \text{for } l \rightarrow 0. \quad (51)$$

This yields for the profile

$$\frac{\Phi(z, 0)}{\Phi(z, \infty)} \simeq -\frac{2}{9 \ln(z/z_0)} \quad \text{for } z \rightarrow \infty, \quad (52)$$

where z_0 is non-universal.

D. Distant wall corrections

Until now the profile near a particle source has been investigated assuming that the particles are extracted by a distant sink located at $z = L$, $L \rightarrow \infty$. In computer simulations only comparatively small systems can be studied and corrections to the profile (45) due to the distant sink become important. At mean field level the profile

which satisfies the boundary conditions $\Phi(0) = \infty$ and $\Phi(L) = -\infty$ is given by

$$\Phi_{\text{mf}}(z) = \frac{2\pi\rho}{gL} \cot\left(\frac{\pi z}{L}\right) = \frac{2\rho}{gz} \left[1 - \frac{1}{3}\left(\frac{\pi z}{L}\right)^2 + \dots\right]. \quad (53)$$

The powers of (z/L) occurring in this expansion below the upper critical dimension can be obtained from a short distance expansion (SDE) of the order parameter field $s(z)$ for $z \rightarrow 0$ [31–33]. The leading term in this SDE (with the lowest momentum dimension) is the unit operator 1. Since $s_s = 0$ due to the Dirichlet boundary condition the next-to-leading contribution is the normal derivative $\rho\partial_n s$. We therefore obtain

$$s(r_\perp, z, t) = A_1 z^{-\sigma} \cdot 1 + A_2 z^{\frac{2-\eta}{2+\eta}} \cdot \rho\partial_n s(r_\perp, t) + \dots \quad (54)$$

The power in front of the normal derivative has been determined by comparing the anomalous scaling dimensions of the individual terms in equation (54),

$$s \sim l^{(d-1+\eta)/2}, \quad \rho\partial_n s \sim l^{(d+3-\eta)/2}, \quad z \sim l^{-(2+\eta)}. \quad (55)$$

The SDE (54) implies that the distant particle sink gives rise to a correction to the profile proportional to $z^{\frac{2-\eta}{2+\eta}} = z^\sigma$ for $z \rightarrow 0$, i.e.

$$\Phi(z) = A_1 z^{-\sigma} \left[1 + B \left(\frac{z}{L}\right)^{2\sigma} + \dots\right]. \quad (56)$$

For $\epsilon = 0$ this form is consistent with the mean field result (53).

The amplitudes A_1 and B depend on the fixed point value of the surface potential, i.e. they take different values for $h_1 = 0$ and $h_1 = \infty$. Equation (53) shows that for $h_1 = \infty$ the (universal) amplitude B is given by $B = -\pi^2/3 + O(\epsilon)$. In the case $h_1 = 0$ with the boundary conditions $\Phi_{\text{mf}}(0) = 0$ and $\Phi(L) = -\infty$ the mean field profile reads

$$\Phi_{\text{mf}}(z) = -\frac{\pi\rho}{gL} \tan\left(\frac{\pi z}{2L}\right) = -\frac{\pi^2\rho}{2gz} \left[\left(\frac{z}{L}\right)^2 + \dots\right]. \quad (57)$$

To determine the amplitude B at leading order in ϵ we divide $\Phi_{\text{mf}}(z)$ by the semi-infinite profile (20) and obtain

$$\frac{\Phi_{\text{mf}}(z)}{\Phi^{[1]}(z)} = \frac{3\pi^2}{2u} (1 + O(u, \epsilon)) \left(\frac{\mu^2 z}{\sqrt{\rho}}\right)^{-\epsilon/2} \left(\frac{z}{L}\right)^2 + \dots \quad (58)$$

At the fixed point $u_* = (2/3)\epsilon + O(\epsilon^2)$ the amplitude B is thus given by $B = 9\pi^2/(4\epsilon) + O(\epsilon^0)$. Note that B is of the order $1/\epsilon$ because the semi-infinite profile vanishes at zero loop order.

VI. SIMULATION RESULTS

In order to check some of the results presented in the previous section by computer simulations we use the standard Monte Carlo technique with Metropolis spin-exchange jump rates on the two-dimensional, driven Ising lattice gas with attractive interactions [1,2]. The driving force is effectively infinity, i.e. every attempt of a particle to jump in the direction of the driving force is successful unless the jump would violate the excluded volume constraint. Jumps in the direction antiparallel to the driving force have zero probability. We use the critical value of the temperature parameter $T_c(\infty) = 1.41T_c(0)$ obtained by Leung [2]. The particle reservoirs at the boundaries are incorporated into the model by a simple change of the updating algorithm: Whenever a boundary site is involved in an updating step the occupation number of this site set equal to a random number $X \in \{0, 1\}$ which is one with probability c_A (at the left boundary) or c_B (at the right boundary). To avoid unwanted correlations each realization of X has to be used for only one update. In the transverse directions periodic boundary conditions are imposed.

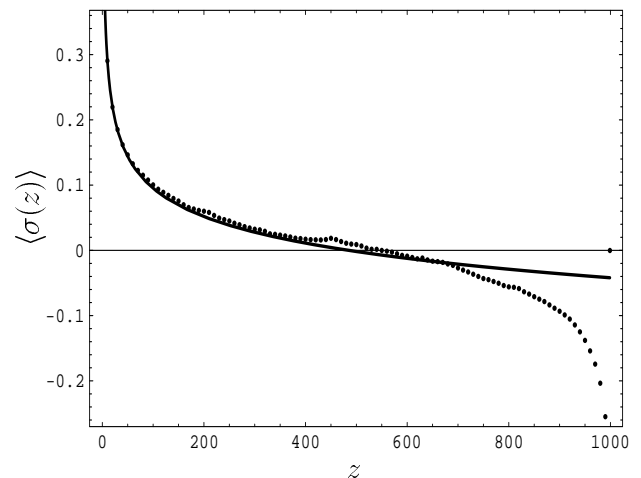


FIG. 3. Density profile for $c_A = 1.0$, $c_B = 0.5$, where the occupation numbers are represented by the spin variable $\sigma = 2n - 1$. The statistical error is everywhere smaller than ± 0.006 . The solid line is a fit using Eq. (56) with $A_1 = 0.678$ and $B = -1.62$.

Fig. 3 shows the density profile for $c_A = 1.0$ and $c_B = 0.5$. The system size is $L_{\parallel} = 1000$ in the direction parallel to the driving force and $L_{\perp} = 500$. At the beginning of each run, an uncorrelated initial state is generated where each lattice site is occupied with probability 0.5. Then 10^5 Monte Carlo steps (per site) are performed to reach the stationary state. The profile shown in Fig. 3 has been obtained by averaging over $2 \cdot 10^5$ configurations. The amplitudes A_1 and B in Eq. (56) have been determined by a least square fit with the result $A_1 = 0.678 \pm 0.004$, $B = -1.6 \pm 0.2$. For this fit

we have used various subintervals of $3 \leq z \leq 50$. (The statistical error in this range is smaller than 0.002.) For larger values of z higher powers in z/L become increasingly important. We have checked that the above values for A_1 and B also provide acceptable fits for smaller systems $[(L_{\parallel}, L_{\perp}) = (500, 397) \text{ and } (125, 250)]$.

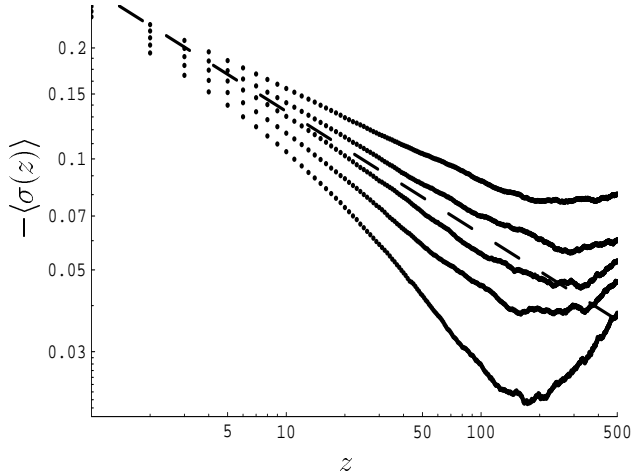


FIG. 4. Double logarithmic plot of the density profile for $c_A = 0.278, 0.280, 0.282, 0.284, 0.286$ (from top to bottom) and $c_B = 0.5$. The spin variable $\sigma = 2n - 1$ has been used. The broken line corresponds to the power $0.29z^{-1/3}$.

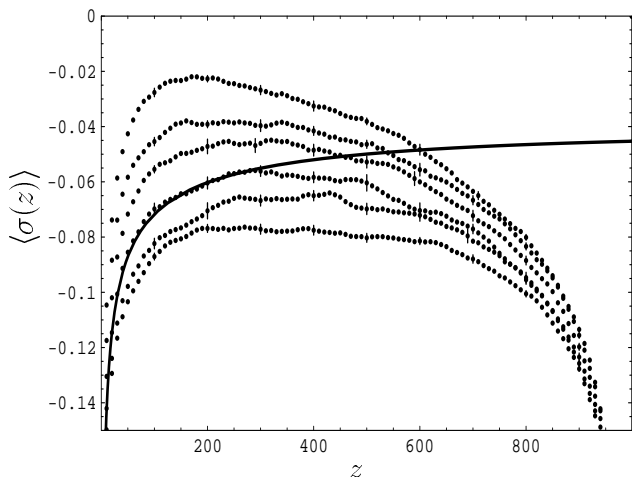


FIG. 5. The density profile for $c_A = 0.278, 0.279, 0.280, 0.282, 0.284, 0.286$ (from bottom to top) and $c_B = 0.5$. The occupation numbers are represented by the spin variable $\sigma = 2n - 1$. The solid curve is a fit using Eq. (56) with $A_1 = -0.30$ and $B = 0.51$.

To determine the amplitude ratio D one first has to find the critical value of c_A that corresponds to a vanishing surface field, $h_1 = 0$. Fig. 4 suggests that this value is close to $c_A \approx 0.28$. For $0.278 \leq c_A \leq 0.282$ we obtained fits consistent with $A_1 = -0.29 \pm 0.02$. One

of these fits is depicted in Fig. 5 together with density profiles for various values of c_A . Each profile is an average over 10^6 configurations. To determine the amplitude B it would be necessary to obtain a more accurate estimate for the critical surface density. The simulation result for the amplitude ratio reads $D = -0.43 \pm 0.03$ which can be compared with our one-loop calculation, $D \approx -\epsilon/9 = -0.33$ for $\epsilon = 3$.

VII. SUMMARY AND OUTLOOK

A particle reservoir coupled to the boundary of a driven diffusive system maintains the critical density in the bulk if the chemical potential of the reservoir is not below a critical value. Above this critical value the density profile (as a function of the distance from the boundary) asymptotically approaches the bulk density from above, where the decay of the profile follows a power law with an exponent σ which can be expressed in terms of the bulk exponent η . At the critical value of the boundary chemical potential the density tends to its bulk value from below. If the chemical potential is close to (but above) its critical value the density profile crosses the critical density at a macroscopic distance ζ from the boundary. The singular power law dependence of the length scale ζ on the boundary chemical potential is characterized by a new exponent ν_1 which has been calculated at first order in $\epsilon = 5 - d$.

While in exclusion models without particle-particle attraction the density profile is always a monotonic function of the distance from the boundary we have shown that in critical DDS stationary profiles can have local maximum points. This is due to the density correlations in the bulk generated (for $d > 1$) by the attractive interaction. If the ‘temperature’ is raised above $T_c(E)$ these correlations survive as long as T is finite. Therefore the *qualitative* form of the density profile will not change for $T_c(E) < T < \infty$.

In this paper one out of a multitude of universality classes describing various types of DDS has been considered. These universality classes differ in the nature of the noise (particle conserving or non-conserving), the presence or absence of quenched disorder and the values of temperature-like critical parameters [34]. We plan to extend the analysis presented here to other universality classes. It is straightforward to derive relations similar to (46) between σ and the anisotropy exponent η for DDS with quenched disorder. This makes it possible to check the field theoretic predictions of Refs. [35,36,34] for disordered DDS by Monte Carlo simulations of the density profile in systems with open boundaries. Note that in the presence of quenched disorder periodic boundary conditions (in the direction parallel to the driving force) may lead to unwanted correlations since the particles are subjected to the same randomness after every passage through the system.

In order to obtain a numerical estimate for the surface exponent ν_1 or a more accurate value for the amplitude ratio D it is necessary to determine the critical surface density more accurately. This is an open problem for future simulations.

ACKNOWLEDGMENTS

This work has been supported in part by the Sonderforschungsbereich 237 [Unordnung und Große Fluktuationen (Disorder and Large Fluctuations)] of the Deutsche Forschungsgemeinschaft.

APPENDIX A: SURFACE DIVERGENCES AT ONE-LOOP ORDER

In order to determine the renormalization constants at one-loop order one has to evaluate the ultraviolet divergent Feynman diagrams shown in Fig. 6. The results have to be interpreted in the distribution sense since the calculation of Green functions involves integrations over the z -coordinates of amputated graphs.

The Laplace transform of the first diagram in Fig. 6 reads

$$-\frac{\lambda g}{2} \int_0^\infty dz e^{-sz} \int_{\mathbf{q}_\perp, \omega} \hat{C}_{\mathbf{q}_\perp, \omega}(z, z) = -\frac{\lambda g}{\epsilon} A_\epsilon \tau^{-\epsilon/2} \times \left(\frac{\tau^2}{\sqrt{\rho} s} + \frac{4\tau}{3} + \frac{2}{3} \sqrt{\rho} s + O(\epsilon) \right), \quad (\text{A1})$$

where $\hat{C}_{\mathbf{q}_\perp, \omega}(z, z)$ is the Gaussian correlator (18) at the Dirichlet fixed point. The two dimensional Laplace transform of the second diagram is given by

$$(\lambda g)^2 \int_0^\infty dz e^{-sz} \int_0^\infty dz' e^{-s'z'} \times \int_{\mathbf{q}_\perp, \omega} \hat{C}_{-\mathbf{q}_\perp, -\omega}(z, z') \partial_{z'} \hat{G}_{\mathbf{q}_\perp, \omega}(z, z') \quad (\text{A2})$$

$$= \frac{\lambda g^2}{2\sqrt{\rho}\epsilon} A_\epsilon \tau^{-\epsilon/2} \left(\frac{2s'}{s+s'} - \frac{2}{3} + O(\epsilon) \right).$$

Applying the inverse Laplace transformation to (A1) and (A2) we obtain

$$\text{Graph 6(a)} = -\frac{\lambda g}{\epsilon} A_\epsilon \tau^{-\epsilon/2} \left(\frac{\tau^2}{\sqrt{\rho}} + \frac{4\tau}{3} \delta(z) + \frac{2}{3} \sqrt{\rho} \delta'(z) + O(\epsilon) \right) \quad (\text{A3})$$

and

$$\text{Graph 6(b)} = \frac{\lambda g^2}{2\sqrt{\rho}\epsilon} A_\epsilon \tau^{-\epsilon/2} \left(2\delta'(z'|z) - \frac{2}{3} \delta(z') \delta(z) + O(\epsilon) \right), \quad (\text{A4})$$

where we have introduced the definition

$$\int_0^\infty dz' \delta'(z'|z) f(z') = -f'(z). \quad (\text{A5})$$

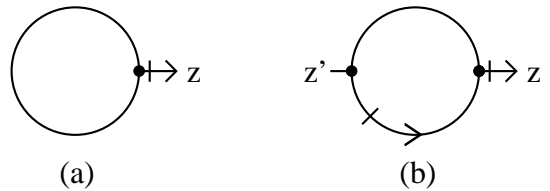


FIG. 6. Ultraviolet divergent Feynman diagrams at one-loop order. A line with (without) an arrow represents the Gaussian propagator (correlator). The short line perpendicular to the propagator line in the diagram (b) indicates a derivative with respect to z' .

The ϵ -poles are canceled by the counter terms (25) and (26) given in section V A. The values of the coefficients A , B , F , K , and Z at one-loop order follow from Eqs. (A3) and (A4) as

$$A = -\frac{1}{\epsilon} \quad B = -\frac{u}{3\epsilon} \quad F = -\frac{4}{3\epsilon} \quad K = \frac{2}{3\epsilon} \quad (\text{A6})$$

and

$$Z = 1 - \frac{u}{\epsilon}. \quad (\text{A7})$$

-
- [1] S. Katz, J. L. Lebowitz, and H. Spohn, Phys. Rev. B **28**, 1655 (1983); S. Katz, J. L. Lebowitz, and H. Spohn, J. Stat. Phys. **34**, 497 (1984).
 - [2] K.-t. Leung, Phys. Rev. Lett. **66**, 453 (1991).
 - [3] H. K. Janssen and B. Schmittmann, Z. Phys. B **64**, 503 (1986).
 - [4] B. Schmittmann and R. K. P. Zia, *Phase Transitions and Critical Phenomena*, edited by C. Domb and J. L. Lebowitz (Academic, London, 1995), Vol. 17.
 - [5] B. Derrida, E. Domany, and D. Mukamel, J. Stat. Phys. **69**, 667 (1992).
 - [6] J. Krug, Phys. Rev. Lett. **67**, 1882 (1991).
 - [7] G. Schütz and E. Domany, J. Stat. Phys. **72**, 277 (1993).
 - [8] B. Derrida, M. R. Evans, V. Hakim, and V. Pasquier, J. Phys. A: Math. Gen. **26**, 1493 (1993).
 - [9] F. H. L. Essler and V. Rittenberg, J. Phys. A **29**, 3375 (1996).
 - [10] D. H. Boal, B. Schmittmann, and R. K. P. Zia, Phys. Rev. A **43**, 5214 (1991).
 - [11] H. W. Diehl, in: *Phase Transitions and Critical Phenomena*, edited by C. Domb and J. L. Lebowitz (Academic, London, 1986), Vol. 10, pp. 75–267.

- [12] H. W. Diehl and S. Dietrich, Phys. Lett. **80A**, 408 (1980);
H. W. Diehl and S. Dietrich, Z. Phys. B **42**, 65 (1981);
Erratum B **43**, 281.
- [13] H. W. Diehl and S. Dietrich, Phys. Rev. B **24**, 2878
(1981).
- [14] H. W. Diehl and S. Dietrich, Z. Phys. B **50**, 117 (1983).
- [15] K. Symanzik, Nucl. Phys. B **190** [FS3], 1 (1981).
- [16] S. Dietrich and H. W. Diehl, Z. Phys. B **51**, 343 (1983).
- [17] H. W. Diehl and H. K. Janssen, Phys. Rev. A **45**, 7145
(1992).
- [18] H. W. Diehl, Phys. Rev. B **49**, 2846 (1994).
- [19] H. K. Janssen and K. Oerding, Phys. Rev. E **53**, 4544
(1996).
- [20] H. K. Janssen, Z. Phys. B **23**, 377 (1976).
- [21] C. De Dominicis, J. Physique (Paris) C **1**, 247 (1976).
- [22] R. Bausch, H. K. Janssen, and H. Wagner, Z. Phys. B
24, 113 (1976).
- [23] C. De Dominicis and L. Peliti, Phys. Rev. B **18**, 353
(1978).
- [24] H. K. Janssen, in: *From Phase Transitions to Chaos,
Topics in Modern Statistical Physics*, edited by G.
Györgyi, I. Kondor, L. Sasvári, and T. Tél (World Sci-
entific, Singapore, 1992), pp. 68–91.
- [25] P. C. Martin, E. D. Siggia, and H. A. Rose, Phys. Rev.
A **8**, 423 (1973).
- [26] U. Ritschel and P. Czerner, Phys. Rev. Lett. **77**, 3645
(1996).
- [27] A. Ciach and U. Ritschel, Nucl. Phys. B **489** [FS], 653
(1997).
- [28] H. W. Diehl, S. Dietrich, and E. Eisenriegler, Phys. Rev.
B **27**, 2937 (1983).
- [29] The integral over the gradient $\partial_{\parallel}\tilde{s}$ (which cancels in a sys-
tem with periodic boundary conditions) can be written
as $\int_V d^d r \partial_{\parallel}\tilde{s} = \int_{\partial V} d^{d-1} r [\tilde{s}(z \rightarrow \infty) - \tilde{s}_s]$. Due to parti-
cle conservation the contribution $\tilde{s}(z \rightarrow \infty)$ may not be
omitted since response functions with $q_{\perp} = \omega = 0$ are
non-zero for $z \rightarrow \infty$.
- [30] M. Benhamou and G. Mahoux, Nucl. Phys. B **305** [FS23],
1 (1988).
- [31] E. Eisenriegler, M. Krech, and S. Dietrich, Phys. Rev.
Lett. **70**, 619 (1993).
- [32] E. Eisenriegler, *Polymers near surfaces* (World Scientific,
Singapore, 1993).
- [33] H. W. Diehl, Int. J. Mod. Phys. B **11**, 3503 (1997).
- [34] V. Becker, PhD thesis, University of Düsseldorf (1997).
- [35] V. Becker and H. K. Janssen, Europhys. Lett. **19**, 13
(1992).
- [36] B. Schmittmann and K. E. Bassler, Phys. Rev. Lett. **77**,
3581 (1996).